Simulation of Vehicle Acoustics In Support of Netted Sensor Research and Development

Carol T. Christou[a] and Garry M. Jacyna[b]

[a]The MITRE Corporation, Department W407, 7515 Colshire Dr. McLean, VA 22102-7508;
[b]The MITRE Corporation, Division W400, 7515 Colshire Dr. McLean, VA 22102-7508

ABSTRACT

The MITRE Corporation has initiated a three-year internally-funded research program in netted sensors, the first-year effort focusing on vehicle detection for border monitoring. An important component is developing an understanding of the complex acoustic structure of vehicle noise to aid in netted sensor-based detection and classification. This presentation will discuss the design of a high-fidelity vehicle acoustic simulator to model the generation and transmission of acoustic energy from a moving vehicle to a collection of sensor nodes. Realistic spatially-dependent automobile sounds are generated from models of the engine cylinder firing rates, muffler and manifold resonances, and speed-dependent tire whine noise. Tire noise is the dominant noise source for vehicle speeds in excess of 30 miles per hour (MPH). As a result, we have developed detailed models that successfully predict the tire noise spectrum as a function of speed, road surface wave-number spectrum, tire geometry, and tire tread pattern. We have also included realistic descriptions of the spatial directivity patterns for the engine harmonics, muffler, and tire whine noise components. The acoustic waveforms are propagated to each sensor node using a simple phase-dispersive multi-path model. A brief description of the models and their corresponding outputs is provided.

1. INTRODUCTION

The Vehicle Acoustic Simulator is an attempt to model the generation and transmission of acoustic energy from a moving vehicle, as part of a Netted Sensors Initiative vehicle classification effort. The simulator consists of several modules as shown in Figure 1.

In the Kinematics module, a set of speed and time waypoints are initially specified. From these, the revolutions per minute (RPM) rates are determined as a function of the vehicle shift speeds, RPM shift points, and the maximum attainable accelerations in each gear. Therefore, RPM rates (cylinder firing rates) are nonlinearly related to vehicle speed and may show rapid fluctuations depending on whether the transmission box is in an up-shift or down-shift mode. In the Engine Harmonics module, the harmonic engine waveforms are generated from realistic physical models based on the engine RPM rates derived in the Kinematics module, from the vehicle trajectory and transmission box gear ratios, the piston settling times, the number of cylinders, and the relative amplitude variations between cylinders.

The Muffler Manifold module generates muffler sounds by bandpass-filtering the engine waveform over a user-specified frequency band and specifying acoustic time delays corresponding to manifold pipe length differences. Tire whine is modeled in a separate module by first passing bandlimited white noise through a proportional bandwidth filter centered around the tread impact harmonics. This generates the tread impact pattern. The tire resonance waveform is determined by first constructing a bandpass filter with an 800-1200 Hz passband response and then passing the tread impact waveform through the filter. Directivity patterns are modeled in a corresponding subroutine, with the muffler directivity pattern approximated by a pipe in an infinite baffle.

The tire whine directivity pattern associated with tire resonance is computed assuming that the tire can be approximated by a randomly vibrating surface of known correlation length, and the engine directivity pattern is approximated by a randomly vibrating plate of known correlation length aligned with the front end of the vehicle. Body occlusions (shadowing) are empirically modeled. Finally, the combined acoustic field at each sensor is calculated in the Propagation module from the propagation time delays for a two-path model.

Further author information: (Send correspondence to C.T.C.)
C.T.C.: E-mail: christou@mitre.org, Telephone: (703) 883-5850
G.M.J.: E-mail: gjacyna@mitre.org, Telephone: (703) 883-6972

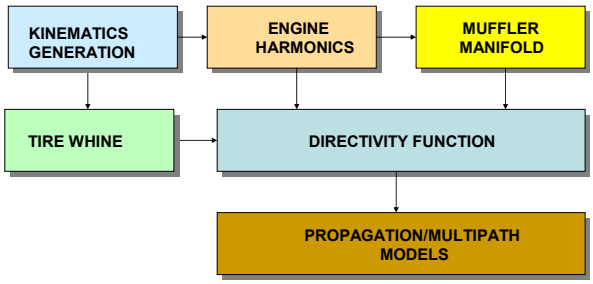

Figure 1. High Fidelity Waveform Simulator.

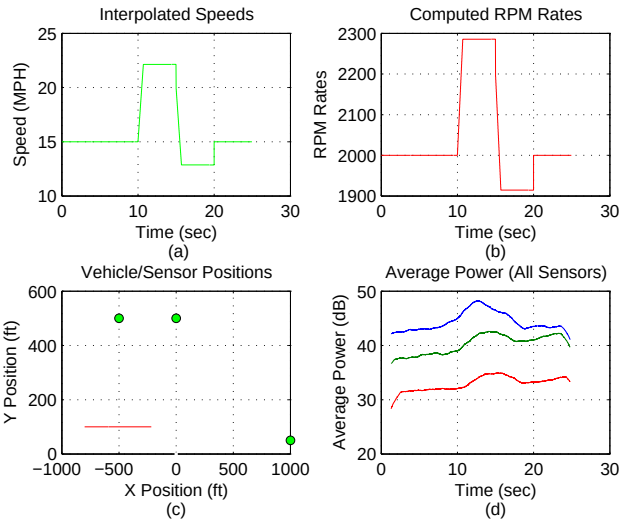

Figure 2. Graphical Output of Kinematics Module.

2. KINEMATICS GENERATION

Two algorithms have been designed to compute kinematic variables (position and speed) versus time for an arbitrary number of vehicles. In the first case, a straight line road model is assumed and in the second, a two dimensional curvilinear model.

In the straight line road model, rectilinear vehicle speeds, displacements, and engine RPM rates are computed from input speed versus time waypoints using a table of transmission shift speeds for known engine RPM set points. Vehicle displacement is then computed from the interpolated speeds given a known initial position for each vehicle. We begin by defining the minimum and maximum speeds for each speed set point, and proceed to determine the interval for each input waypoint speed, beginning with the first. If the kth speed is greater than the current interval, we upshift to the required speed, determine the time to reach the upper set point, and compute the speed and engine RPMs up to the upper set point. If the kth speed is less than the current interval, we downshift to the required speed, determine the time to reach the lower set point, and trap the engine RPM at zero vehicle speed. Finally, if the kth speed is within the current interval, no shifting is required. If the preset speed is reached before the end of the time interval, then that speed is maintained to the end of interval. Otherwise, the time interval is extended to accommodate the speed while preserving the interval time differences. We then accumulate all vehicle speeds, all engine RPM rates and compute the vehicle displacements. Example results are presented in Figure 2. Subplot 2a is a graph of speed versus time, subplot 2b a graph of RPM rates versus time. Subplot 2c shows the rectilinear path of a car starting at x = −800 ft, y = 100 ft (red line), with the green dots marking the sensor positions. Subplot 2d shows the final simulator output, the received power at the three sensors.

In the curvilinear road model, we begin by choosing the x and y coordinates of a predefined number of waypoints. The best option for defining the trajectory* of the vehicle is to outline the road shape by fitting a cubic spline to the waypoints. We define the speeds at the waypoints and solve for the corresponding times, given the arclengths between points. After fitting a cubic spline to the waypoints and choosing the corresponding speeds, the radius of curvature R, length L and maximum safe speed for each road segment are computed from

*Strictly speaking, a path is a geometric representation in space, while a trajectory is a path with a velocity-time profile.

the first and second derivatives for each sampled time along the spline curve:

$$\begin{aligned} R(k) &= \frac{1}{N(k)} \sum_{i=1}^{N(k)} \frac{(1+\Delta_i^2)^{\frac{3}{2}}}{|\Delta\Delta_i|}; \\ L(k) &= \sum_{i=1}^{N(k)} \sqrt{1+\Delta_i^2}\, dx_i; \\ v_{turn} &= \sqrt{g f_s R(k)} \end{aligned} \tag{1}$$

where $\Delta \equiv dy/dx$, $\Delta\Delta \equiv d^2y/dx^2$, $N(k)$ = number of time points in the kth road segment,[†] g is the acceleration of gravity = 32.2 ft/sec^2, and f_s = coefficient of static friction.[‡] The following steps are then performed:

a. If the preset speeds exceed the safety limit at each waypoint, then they must be decreased: $v(k) = \min(v(k), v_{turn}(k))$, for the kth waypoint.

b. Obtain rough estimates of the final times t_f for each segment k based on the length $L(k)$ and the average speed in that segment: $.5(v_{initial} + v_{final})$. The initial time of motion in each road segment is the final time for the previous segment.

c. Find the tangents and the v_x, v_y components at the end points of each segment. Plan the trajectory using cubic polynomials for the x and y coordinates as functions of time:

$$\begin{aligned} x(t) &= a_{0,x} + a_{1,x}t + a_{2,x}t^2 + a_{3,x}t^3; \\ y(t) &= a_{0,y} + a_{1,y}t + a_{2,y}t^2 + a_{3,y}t^3; \end{aligned} \tag{2}$$

d. Calculate the coefficients of the cubic polynomials, given the coordinates and velocity components at the endpoints of the road segment and the tentative times t_i and t_f. Differentiate the polynomials twice to get the first and second derivatives $v_x(t)$, $v_y(t)$, $a_x(t)$, $a_y(t)$.

e. Check that the speeds $v(t)$ do not exceed the maximum safe speeds inside each road segment and that the accelerations do not exceed the maximum acceleration for the corresponding gear. If these conditions are not met, lower the input speeds at the waypoints and start again.

f. Find the cumulative displacements for each segment from the speed components, and check on agreement with $L(k)$ in Eq. (1). Also, check agreement of estimated waypoints with original waypoints. Figure 3 shows some example results, in which we see that the calculated displacements agree perfectly with the spline fit to the waypoints.

3. VEHICLE SOUND SOURCES

Vehicles are complex systems made up of many different parts, and have natural frequencies that result from a combination of their components' natural frequencies. The total acoustic signal from a vehicle contains contributions from the engine, the exhaust, the tire-road surface interaction, the transmission system, fan, air intake, etc.[1] In this work, we model three sources: engine, muffler and tire noises.

The engine harmonics and filtered muffler sounds are generated based on the number of cylinders N_c, piston transient settling time T_p, the normalized ratios η, the relative piston ping amplitudes a, the engine RPM rates, the muffler bandpass frequencies F_m, and the relative propagation time delays Δt through the manifold pipes (one per cylinder) and muffler baffles. From these quantities the engine waveform vectors, the manifold waveform vectors and the vector of average engine/muffler amplitudes are calculated.[2]

[†]To make for greater smoothness and ease of computation, waypoints should be spaced not more than $\approx$ 500 ft apart.

[‡]On a level road, static friction provides a centripetal force $\frac{mv^2}{R} = mgf_s$, which can be solved for v_{turn}.

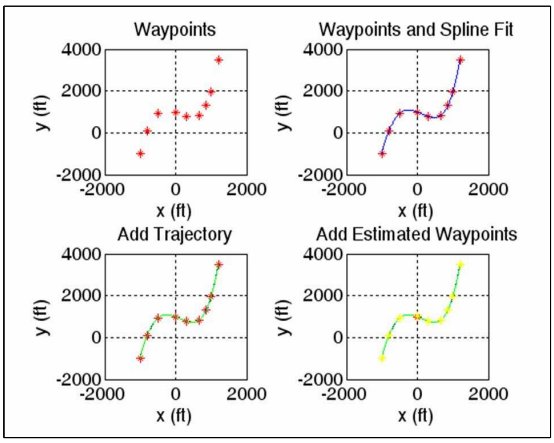

Figure 3. Curvilinear Road Model.

3.1. Engine Waveforms

3.1.1. Basics

Assuming a periodic piston ping waveform $s(t-nT)$, the time-series acoustic signal generated by the engine may be written as

$$x(t) = \sum_{n=-\infty}^{\infty} a(n)s(t-nT), \tag{3}$$

where T is the constant piston ping period, and $a(n)$ are the individual cylinder weights. Evaluating the Fourier transform of this expression yields

$$X(f) = S(f) \sum_{n=-\infty}^{\infty} a(n) \exp(-2\pi i f n T), \tag{4}$$

where f is the frequency. The piston ping period is related to the RPM rate by $T = \frac{120}{N_c RPM}$, where it is assumed that only half the cylinders fire per revolution. Now, $a(n) = \tilde{a}(j)$, $j = \mathrm{mod}(n, N_c)$, where N_c is the number of cylinders, and $\widetilde{a}(j)$ $(0 \le j \le N_c - 1)$ are the cylinder weights. Thus, $a(n)$ is N_c-periodic, and $a(n)$, $X(f)$ may be written as

$$\begin{aligned} a(n) &= \frac{1}{N_c} \sum_{j=0}^{N_c-1} \tilde{A}(j) \exp(2\pi i \frac{jn}{N_c}), \\ X(f) &= \frac{1}{N_c} S(f) \sum_{j=0}^{N_c-1} \tilde{A}(j) \sum_{n=-\infty}^{\infty} \exp(-2\pi i (fT - j/N_c)n), \end{aligned} \tag{5}$$

where $\tilde{A}(j)$ is the discrete Fourier transform (DFT) of $\tilde{a}(j)$. Let us look at the expression $\sum_{n=-\infty}^{\infty} \exp(-2\pi i (fT - j/N_c)n) = \sum_{n=-\infty}^{\infty} \exp(-2\pi i \widetilde{f} T n)$, where $\widetilde{f} \equiv f - \frac{j}{N_c T}$. The DFT is

$$\begin{aligned} \Gamma(\widetilde{f}) &= \sum_{n=-\infty}^{\infty} c_n \exp(-2\pi i \widetilde{f} T n), \qquad \text{where} \\ c_n &= T \int_{\frac{-1}{2T}}^{\frac{1}{2T}} \Gamma(\widetilde{f}) \exp(2\pi i \widetilde{f} n T) d\widetilde{f}. \end{aligned} \tag{6}$$

If $\Gamma(\widetilde{f}) = \delta(\widetilde{f})/T$, then

$$\frac{\delta(\widetilde{f})}{T} = \sum_{n=-\infty}^{\infty} \exp(-2\pi i \widetilde{f} n T); \qquad \frac{-1}{2T} \leq \widetilde{f} \leq \frac{1}{2T}. \tag{7}$$

Since the series is periodic in $1/T$, we can extend $\widetilde{f}$ to $-\infty \leq \widetilde{f} \leq \infty$, so that $\sum_{n=-\infty}^{\infty} \exp(-2\pi i \widetilde{f} n T) = \frac{1}{T} \sum_{r=-\infty}^{\infty} \delta(\widetilde{f} + \frac{r}{T})$. Inserting into Equation (5), we get

$$X(f) = \frac{1}{N_c T} \sum_{r=-\infty}^{\infty} \Big[\sum_{j=0}^{N_c-1} \tilde{A}(j) S(j/N_c T - r/T) \delta(f - j/N_c T + r/T) \Big], \tag{8}$$

which represents a series of periodic narrowband lines. To estimate $s(t)$, we begin with a simple spring-dash pot system of mass m, spring constant k, damping coefficient γ, and an applied force $f(t)$, the equation of motion $m\ddot{s}(t) + \gamma \dot{s}(t) + ks(t) = f(t)$ generates the underdamped piston transients in the time domain as:

$$\begin{aligned} s(t) &= \sin\left(\beta \frac{t}{T_p}\right) \exp\left(-\frac{t}{T_p}\right); \qquad t \geq 0; \\ \beta &= \frac{\sqrt{(1-\eta^2)}}{\eta}, \end{aligned} \tag{9}$$

where η is the normalized damping factor $\eta = \frac{\gamma/2m}{\sqrt{k/m}}$. Fourier transforming the above expression for $s(t)$ and inserting into Eq. (8), we may estimate the narrowband engine spectrum $X(f)$. Figure 4 is an example of a harmonic line spectrum for a six cylinder engine with constant period $T = .01$ sec, $T_p = .0015$ sec, $\eta = .4$, and cylinder amplitudes $A_c = [1,\ 2,\ 4,\ 5,\ 7,\ 3]$. The six series are distinguished by their color and correspond to motion of the different cylinders.

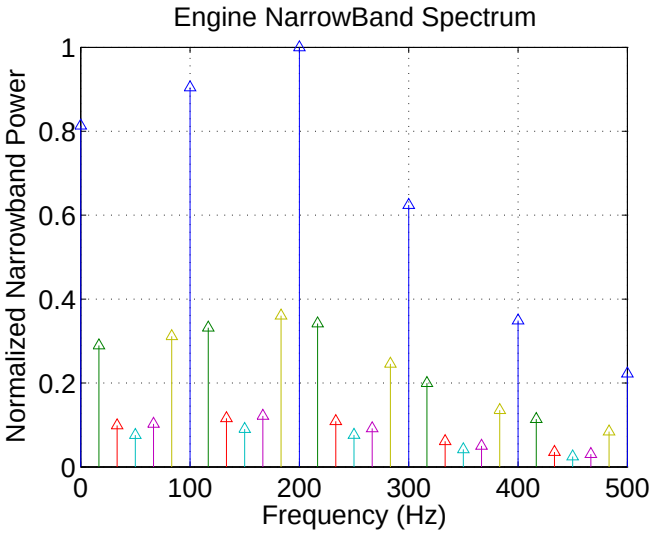

Figure 4. Narrowband Engine Spectrum for Constant Period T.

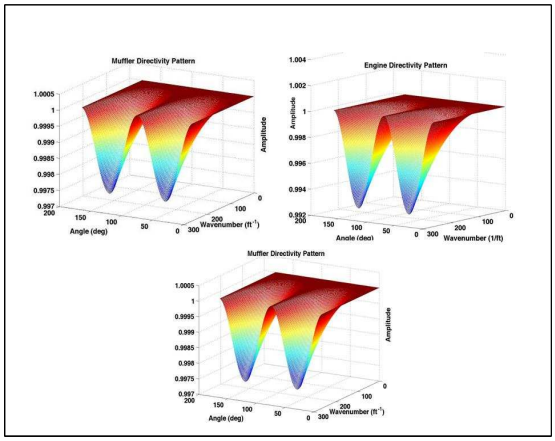

Figure 5. Beam Patterns for the Muffler, Engine and Tire Waveforms.

In general, the piston ping period is a function of time so that Equation (3) is no longer strictly valid. A more generalized form of Equation (3) is:

$$x(t) = \sum_{n=0}^{\infty} a(n) s(t - t_n), \tag{10}$$

where $t_n = \sum_{j=0}^{n} T(t_j)$. Each off-set time is computed by determining the corresponding fixed point of the equation.[§] The engine waveform $x(t)$ is then scaled by a precomputed value ζ_{engine} based on the characteristics of the engine and the amount of acoustic absorption by the vehicle frame:

$$x_{engine}(t) = \zeta_{engine} x(t). \tag{11}$$

3.2. Muffler Waveforms

A muffler is an example of a simple bandpass filter. Each engine cylinder is linked to the muffler through an exhaust manifold of variable length. The acoustic waveform at the output of the jth pipe can be represented by:

$$y_j(t) = \widetilde{a}(j-1) \sum_{n=-\infty}^{\infty} s(t - (j-1)T - nN_cT - \Delta_j), \tag{12}$$

where Δ_j are the individual pipe time delays and the piston ping period T is assumed constant. The input to the muffler can be expressed by $Z(t) = \sum_{j=1}^{N_c} y_j(t)$. Similarly, the output acoustic waveform from the muffler can be written as

$$m(t) = h(t) \otimes Z(t) = \sum_{j=1}^{N_c} h(t) \otimes y_j(t), \tag{13}$$

where $h(t)$ is the impulse function corresponding to a bandpass filter approximation to a muffler, and the symbol $\otimes$ denotes a convolution operation. In general, the piston ping period T is a function of time, so appropriate adjustments to equation (12) are required in a manner similar to Equation (10). Finally, the muffler waveform $m(t)$ is scaled by $\zeta_{muffler}$ based on the particular characteristics of the muffler:

$$x_{muffler}(t) = \zeta_{muffler} m(t). \tag{14}$$

3.3. Tire Noise

Tire noise is a complicated phenomenon which is a function of speed and tread pattern pitch for a periodically recurring tread pattern.[34] Tire noise consists of two components: a tread impact mechanism (tread in contact with the road surface) and a broadly peaked resonance pattern that includes such physical effects as tire resonance, Helmholtz cavity resonance, and Aeolian tones generated by vortex shedding off the tire. The Helmholtz cavity resonance is typically referred to as the Horn effect. The waveforms are generated by first passing bandlimited white noise through a (triangular) proportional bandwidth filter centered around the tread impact harmonics. This generates the tread impact pattern. The resonance pattern is determined by first constructing a bandpass filter with a pass band in the range 800-1200 Hz and then passing the previously computed tread impact waveform through the filter. A resonance peak is formed only when the tread impact waveform is within the frequency pass band of the bandpass filter. This typically occurs at speeds in excess of 30 MPH. Two waveforms are output: x_{tire} is the (omnidirectional) tread impact waveform and $x_{resonance}$ is the directional tire resonance waveform. An amplitude correction factor is used to adjust the noise level as a function of vehicle speed. To summarize:

$$x_{tire}(k) = \zeta_{tire} A_k h(k) \otimes w(k), \tag{15}$$

where $h(k)$ is the tread impact filter:

$$h(k) = \text{real}\left[\sum_j w_j H_0(k,j) \sum_n x_n \exp(2\pi i n v_k t_j / S_0)\right], \tag{16}$$

[§]For variable engine speeds, T is a function of time. Let $t_s = t - T(t)$. Since $s(t_s) = 0$ for $t_s < 0$, we want to find t such that $t_s = 0$, i.e., $t = T(t)$ is the first fixed point t_1. For $t \in [a,b]$ and $T(t) \in [a,b]$ such that $T(t)$ has continuous first derivatives, assume $T(t)$ has a fixed point. Also, if $|T'(t)| \leq K$ exists and $K < 1$, then $T(t)$ has a unique fixed point. We can find the fixed point through iteration: Let p be the fixed point, and let $t_n = T(t_{n-1})$, $|t_n - p| = |T(t_{n-1}) - T(p)| = |T'(\xi)||t_{n-1} - p| \leq K|t_{n-1} - p|$ where ξ is an intermediate point between t_{n-1} and p. By induction, $|t_n - p| \leq K^n |t_0 - p|$. As $n \to \infty$, $|t_n - p| \to 0$, so $p = \lim_{n\to\infty} T(t_n)$. Since $|T'(t)| = 120\frac{|RPM'(t)|}{N_c RPM^2(t)}$, we require $|T'(t)| \leq K < 1$, so that the iteration converges. More generally, for the Kth spike: $t^{(k)} = T(t^{(k)}) + T(t^{(k-1)})$; $T_0 = 0$. A similar inductive argument leads to the same iterative procedure outlined above.

and $H_0(k,j)$ is the proportional bandwidth filter:

$$H_0(k,j) = \frac{[\sin(\pi v_k t_j / S_0)]^2}{(\pi v_k t_j / S_0)^2}, \tag{17}$$

A_k is a speed-dependent amplitude term $A_k = (v_k/v_0)^{P_{tire}/20}$, $x_n \equiv 1/(1+n^2)$, ζ_{tire} is a (constant) predetermined amplitude correction, v_k is the vehicle speed at time index k t_k, v_0 is a reference speed, S_0 is the tread pattern pitch, $t_j = -.5 + (j-1)/F_s$; $1 \le j \le 1 + F_s$, P_{tire} is a predetermined power-law factor, w_j are Hanning weights, and $w(k)$ is bandlimited Gaussian white noise. The expression for $x_{resonance}(k)$ is similar to Equation (15), except that $w(k)$ is the horn/resonance waveform and the normalization constant ζ_{tire} is different.

4. DIRECTIVITY PATTERNS

In this module, the appropriate input waveforms are filtered by the engine, exhaust, and tire whine frequency-dependent directivity patterns. The exhaust directivity pattern is approximated by a pipe in an infinite baffle. The tire whine directivity pattern associated with tire resonance is modeled by a vibrating surface of known correlation length, and the engine directivity pattern is modeled as a randomly vibrating plate with known correlation length. Acoustic occlusions (car frame, etc.) are approximated by an empirically-derived shadow zone model. The outputs are $[180 \times N']$ filtered output waveforms (180 bearings spaced 2 degrees apart), where N' is slightly smaller than the number of time samples as a result of the filter time delay.

The muffler beampatterns are computed as

$$\begin{aligned} B_0(\theta,u) &= 2\frac{J_1(k(u)R_p\sin(\theta))}{kR_p\sin(\theta)}; \qquad -180^\circ \le \theta \le 180^\circ; \\ k(u) &= 2\pi\frac{F_s}{cN_{FFT}}u; \qquad u = \left[0, ...\frac{N_{FFT}}{2}\right], \end{aligned} \tag{18}$$

where N_{FFT} is the FFT size, c = 1100 ft/sec is the speed of sound in air, R_p is the effective pipe exhaust radius in feet, $k(u)$ represents the wavenumber at time u, and J_1 is the Bessel function of the first kind of order one. The empirically derived shadow zone is described by

$$Shadow_0 = \exp(-\alpha|\theta - 90^\circ|); \qquad |\theta| > 90^\circ, \tag{19}$$

where α is the empirical shadow zone parameter (set equal to .1 here, but always less than 1). We then compute the spatial impulse response function given the beampattern, filter the waveforms and finally correct for the filter delay.

For tire noise, we let $-90^\circ \le \theta \le 270^\circ$, and calculate the beampattern for a random surface:

$$B(\theta,u) = \exp((.5k(u)L_c\sin(\theta))^2), \tag{20}$$

where L_c is the front frame/tire correlation distance in feet. The engine beampattern (random surface) is the same as Equation (20), except than $\theta \le 180^\circ$. An empirically derived shadow zone is also applied in this case for $|\theta| \le 180^\circ$. Again, we compute the beam impulse response and filter the waveforms. Figure 5 shows the directivity patterns for the muffler, engine and tire waveforms, respectively. For notational convenience, the filtered waveforms $x_{engine}(t)$, $x_{muffler}(t)$, $x_{tire}(t)$, and $x_{resonance}(t)$ are denoted by W_{engine}, $W_{muffler}$, and W_{tire} (x_{tire} and $x_{resonance}$ are combined to form the composite tire waveform).

5. PROPAGATION MODEL

The next step in the simulation process is to compute the individual waveforms at each sensor based on a simple direct and reflected ray multipath model. Micromultipath effects are modeled by a unit modulus phase dispersive filter, while travel times include corrections for source motion (Doppler) relative to the individual sensors. The vehicle displacements and sensor positions are input from the Kinematics module.

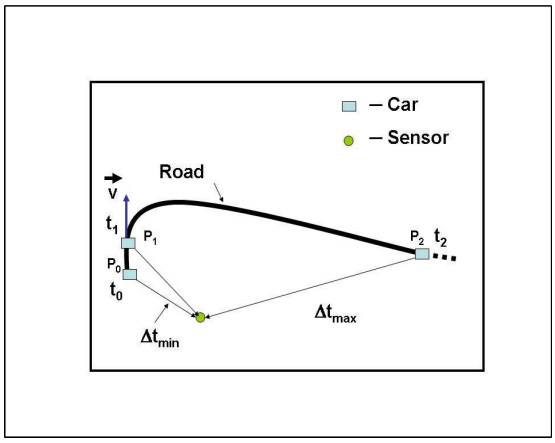

Figure 6. Car Motion Along a Road.

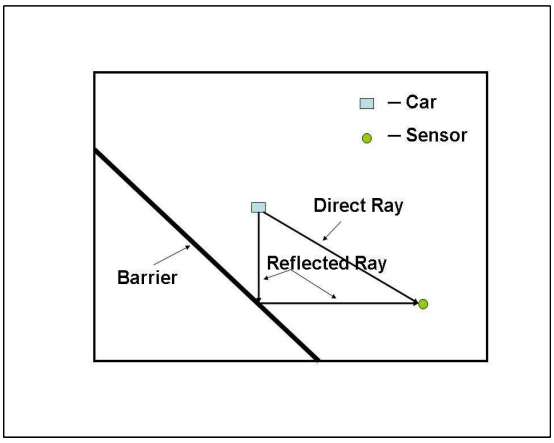

Figure 7. Geometry of Signal Transmission.

The vehicle may trace out a straight line or curvilinear trajectory with initial position X_0, Y_0. A reflecting wall is optional and may be located anywhere. Figure 6 shows a diagram of a hypothetical car moving along a curvilinear road. Start time for the car's motion is t_0, and we assume a number of total time samples equal to $F_s(t_2 - t_0)$, where t_2 is the end time. Suppose the minimum time delay t_{min} for an acoustic signal to reach the sensor corresponds to time t_0 at point P_0 on the road, and that the maximum delay t_{max} corresponds to point P_2 at time t_2. The signal from the car at time t_0 doesn't reach the sensor until time $t_1 = t_0 + t_{min}$, when the car is at position P_1. Likewise, the signal from time t_2 doesn't reach the sensor until some time after the vehicle has stopped. It is, therefore, necessary to incorporate these delays, equivalent to phase differences, into the waveforms that are provided by the directivity function. Figure 7 shows the geometry of signal transmission between car and sensor when there is an arbitrarily placed reflecting barrier in the vicinity of the vehicle's motion. There are two rays, a direct and a reflected one, to which Snell's law applies.

In order to calculate the respective time delays t_D and t_R, we refer to Figure 8: Here, C represents the position of the car, S the sensor position and C' the position of the mirror image of the point C through the plane of the barrier. The point O denotes the intersection of the incident ray CO with the mirror plane, X_B is the intersection of the barrier with the x axis and Y_B its intersection with the y axis. The direct path length is easily seen to be:

$$|\Delta\overrightarrow{R}_D| = \overrightarrow{CS} = \sqrt{\Delta x_D^2 + \Delta y_D^2}; \quad \Delta x_D = x_S - x_C, \;\; \Delta y_D = y_S - y_C. \tag{21}$$

The reflected path length may be calculated by noting that $C'S = CO + OS$. Simple geometry considerations lead us to the following expressions:

$$\begin{aligned} |\Delta\overrightarrow{R}_R| &= C'S = \sqrt{\Delta x_R + \Delta y_R}; \\ \Delta x_R &= -(x_S - X_{C'}) = -x_S + x_C - 2\ell\frac{Y_B}{L}; \\ \Delta y_R &= -(y_S - y_{C'}) = -y_S + y_C - 2\ell\frac{X_B}{L}; \\ \ell &= L_1 \sin\phi; \;\; \phi = \arccos\Big(\frac{L^2 - L_1^2 - L_2^2}{2L_1L_2}\Big), \end{aligned} \tag{22}$$

where ℓ is the perpendicular distance of point C from the barrier plane. The corresponding time delays are $\Delta t_D = \Delta R_D/c$, $\Delta t_R = \Delta R_R/c$. This is repeated for all waveform time samples. Figure 9 shows the calculation

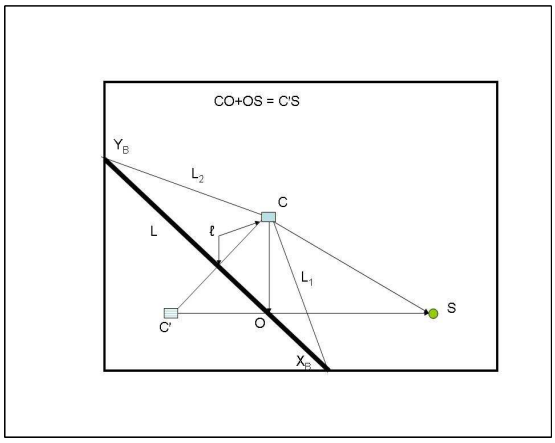

Figure 8. Calculation of Direct and Reflected Path Time Delays.

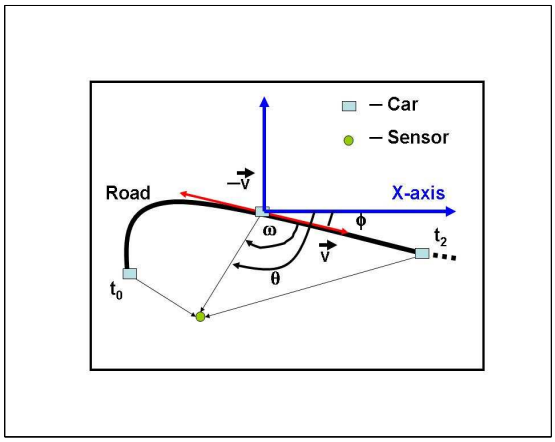

Figure 9. Calculation of the Velocity-Sensor Angle.

of the course angle ω, measured positive counterclockwise from the velocity vector to the car-sensor vector (direct path). The angle θ is the bearing of the direct path vector measured from the x-axis counterclockwise. The angle ϕ is the bearing of the velocity vector, and $\omega = \theta - \phi$. The bearings for the direct path (θ_D), reflected path (θ_R), and the velocity vector (ϕ_v) are simply

$$\theta_D = \arctan\left(\frac{\Delta y_D}{\Delta x_D}\right); \quad \theta_R = \arctan\left(\frac{\Delta y_R}{\Delta x_R}\right); \quad \phi_v = \arctan\left(\frac{v_y}{v_x}\right) \tag{23}$$

where the signs of the x and y coordinates must be taken into account to assign the correct quadrant. The relative course angles ω are then converted to indexed beams, since the waveform directivity patterns are given at intervals of two degrees. Direct and reflected path spreading losses are calculated as:

$$Spread_D = \frac{R_0}{c\Delta t_D}; \quad Spread_R = \frac{R_0}{c\Delta t_R}, \tag{24}$$

where R_0 is reference range of 3 ft. We then add together the three waveforms after weight normalizing by the components of β:

$$U(t) = \beta(1)W_{Engine}(t) + \beta(2)W_{Muffler}(t) + \beta(3)W_{Tire}(t). \tag{25}$$

where β is a three-component vector of relative engine/muffler/tire component amplitudes. We define V as the matrix U adjusted for the time delays. Since the waveforms W_{Engine}, $W_{Muffler}$ and W_{Tire} are read in as $180 \times N'$ matrices, we must index into them to find the waveform corresponding to the correct bearing for each time. After multiplying by the spreading factor

$$Z_D(m,t) = Spead_D V(m,t); \quad Z_R(m,t) = \alpha Spread_R V(m,t), \tag{26}$$

where m is the sensor number, t is the time, and α is the reflectivity loss parameter (set equal to .5 here, but always ≤ 1), we finally filter the waveforms and combine paths to get the received waveforms:[¶]

$$Z(m,t) = -filter(b_d, a_d, Z_D) - filter(b_r, a_r, Z_R), \tag{27}$$

where $a_d = [1 - Diffuse_d]$, $b_d = -a_d$ are the diffuse direct path filter coefficients, while $a_r = [1 - Diffuse_r]$, $b_r = -a_r$ are the diffuse reflected path filter coefficients. $Diffuse_d$ is a dispersive direct path parameter between 0 and 1, and $Diffuse_r$ is a dispersive reflected path parameter betwwen 0 and 1.

[¶]Note that $filter(b_d, a_d, Z_D)$ describes an ARMA filter with vector coefficients b_d and a_d.

6. RESULTS AND CONCLUSIONS

Some example simulator outputs are presented in Figures 10-13. In this case, there were three sensors at positions $(-500, 500)$, $(0, 500)$ and $(1000, 50)$. Figure 10 shows the positions, speeds and RPMs of the vehicle, as well as the received powers at the sensors. The sampling rate was chosen as 4000 Hz, which allows the tire hum around

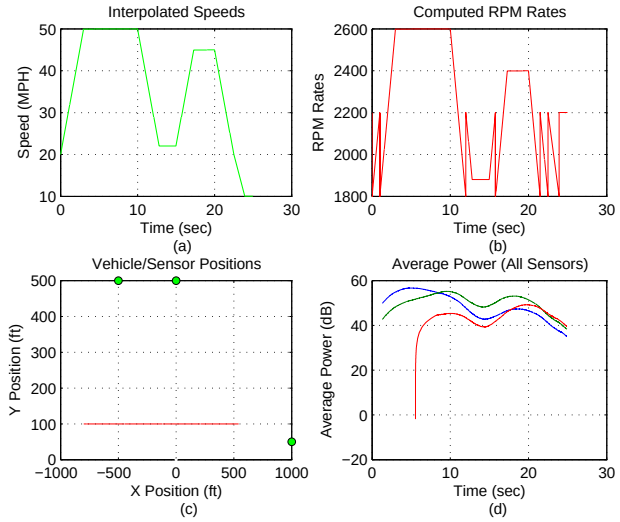

Figure 10. Simulator Results: Positions, Speeds, RPMs, Powers at Sensors.

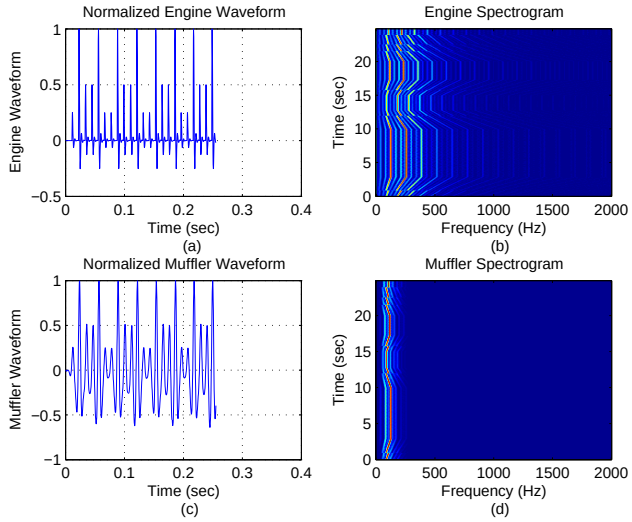

Figure 11. Simulator Results: Engine and Muffler Waveforms and Spectrograms.

900-1000 Hz to be observed in Figure 12. Figure 11 contains the simulated engine and muffler waveforms and spectrograms. We see that the engine spectrum (subplot 11b) is dominated by a group of narrowband lines below 500 Hz. The muffler spectrum (subplot 11d) features a couple of strong lines around 100 Hz.

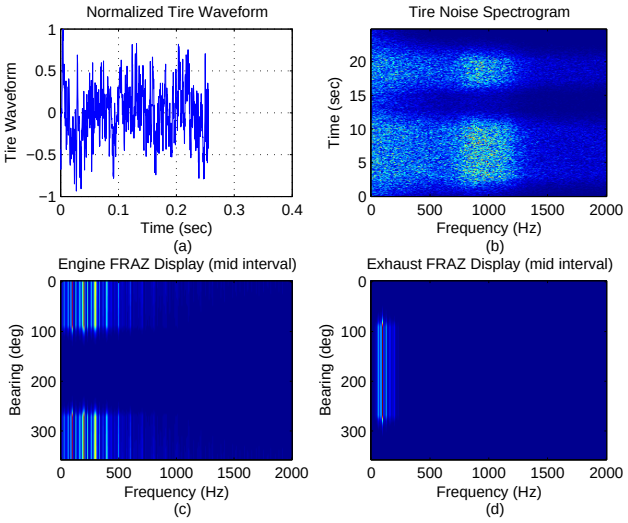

Figure 12. Simulator Results: Waveform, Spectrogram and FRAZ Displays.

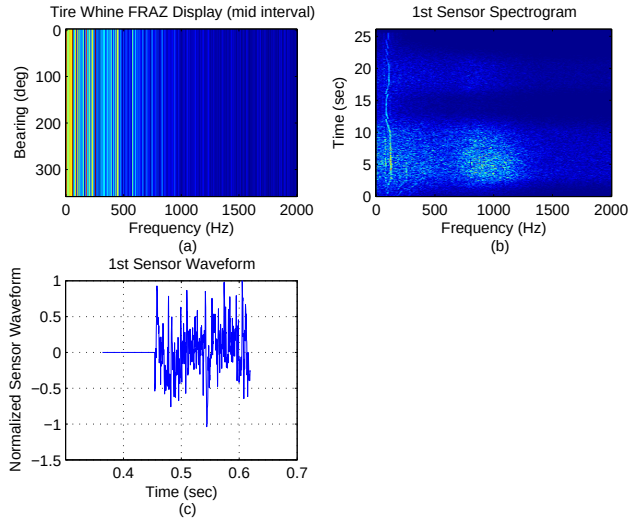

Figure 13. Simulator Results: Tire Whine FRAZ Display and Sensor Spectrogram.

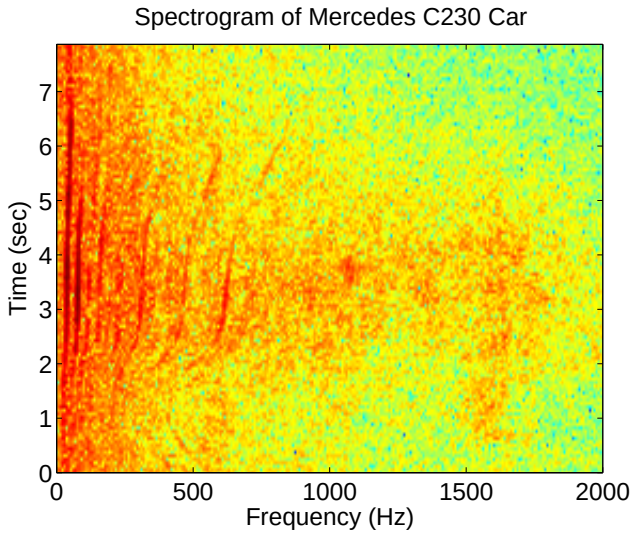

Figure 14. Real Data: Spectrogram of a Mercedes C230 Car.

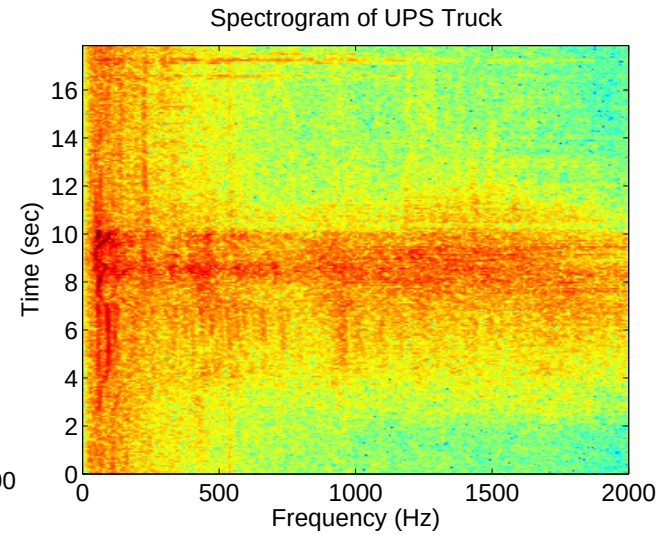

Figure 15. Real Data: Spectrogram of a UPS Truck.

The tire noise spectrum in Figure 12 exhibits broadband properties with the tire hum around 900-1000 Hz clearly visible. The engine and muffler frequency-azimuth (FRAZ) displays in the same figure exhibit low frequency narrowband lines, while the tire whine FRAZ display in Figure 13 has more broadband characteristics extending to higher frequencies. The received spectrogram at the first sensor in the same figure contains visible contributions from engine narrowband components and broadband noise from the tires. The spectrograms for the other sensors are similar. Figures 14 and 15 are spectrograms of real data collected on the MITRE campus. Figure 14 shows a Mercedes C230 car spectrogram, with strong narrowband lines below $\sim$ 500 Hz and a pronounced Doppler effect arising from motion speedup, as evidenced by a noticeable shift of the line series beginning around $T = 2$ sec. There is also indication of tire hum around 1000 Hz. Figure 15 shows the spectrogram of a UPS truck, with a dominant broadband component between 8 and 10 seconds, when it was probably speeding up. There are narrowband lines below $\sim$ 200 Hz, which start exhibiting Doppler effects around 8 seconds, although not as pronounced as those of the car. Comparison of these two figures with Figures 11b, 12b and 13b shows that our model has essentially captured the main components of vehicle acoustic signatures.

In summary, we have attempted to model vehicle acoustic noise by simulating engine and muffler sounds, which contain primarily harmonic line series, and tire noise which at higher speeds is dominated by broadband tire hum. The computed waveforms are functions of the RPM rates, which in turn depend on the kinematic parameters of the vehicle. The waveforms are filtered, time delayed and propagated to the sensor positions using a phase dispersive two-path model.

REFERENCES

1. A. Crewe, et al., "Sound Decomposition-A Key to Improved Sound Simulation", paper no. 2003-01-1423, Society of Automotive Engineers, 2003.
2. M. Bodden and R. Heinrichs, "Analysis of the Time Structure of Gear Rattle", Proceedings of the Internoise 99, pp. 1273-1278, Fort Lauderdale, FL, 1999.
3. U. Sandberg and J. A. Ejsmont, "Noise Emission, friction and rolling resistance of car tires-Summary of an experimental study", Proceedings of the 2000 National Conference on Noise Control Engineering, Newport Beach, CA, December 3-5, 2000.
4. U. Sandberg, "The Multi-Coincidence Peak around 1000 Hz in Tyre/Road Noise Spectra", Euronoise Conference, paper ID 498, Naples, 2003.